

FUSE OBSERVATIONS OF INTERSTELLAR GAS TOWARDS THE LMC STAR SK -67 05

S.D. FRIEDMAN¹, J.C. HOWK¹, B-G ANDERSSON¹, K.R. SEMBACH¹, T.B. AKE¹, K. ROTH¹, D.J. SAHNOW¹, B.D. SAVAGE², D.G. YORK³, G. SONNEBORN⁴, A. VIDAL-MADJAR⁵, E. WILKINSON⁶

Draft version October 25, 2018

ABSTRACT

We report on measurements of interstellar O VI, H₂, P II, Si II, Ar I, and Fe II absorption along the line of sight to Sk -67 05, a B0 Ia star in a diffuse H II region in the western edge of the Large Magellanic Cloud (LMC). We find $\log N(\text{O VI}) = 14.40 \pm 0.04$ in the Milky Way (MW) component and, using the C IV column density from previous IUE observations, $N(\text{C IV})/N(\text{O VI}) = 1.00 \pm 0.16$, a value similar to other halo measurements made with *FUSE*. In the LMC component, $\log N(\text{O VI}) = 13.89 \pm 0.05$, and $N(\text{C IV})/N(\text{O VI}) < 0.4$ (3σ), since only an upper limit on $N(\text{C IV})$ is available. Along this sightline the LMC is rich in molecular hydrogen, $\log N(\text{H}_2) = 19.50 \pm 0.08$; in the MW $\log N(\text{H}_2) = 14.95 \pm 0.08$. A two-component fit for the excitation temperature of the molecular gas in the LMC gives $T_{01} = 59 \pm 5$ K for $J = 0, 1$ and $T_{ex} = 800 \pm 330$ K for $J = 3, 4, 5$. For the MW, $T_{01} = 99^{+30}_{-20}$ K; no excitation temperature could be determined for the higher rotational states. The MW and LMC gas-phase [Fe/P] abundances are ~ 0.6 and ~ 0.7 dex lower, respectively, than solar system abundances. These values are similar to [Fe/Zn] measurements for the MW and LMC towards SN 1987A.

Subject headings: galaxies: Milky Way, LMC – ISM:atoms – ultraviolet:ISM

1. INTRODUCTION

The analysis of interstellar absorption lines provides fundamental information about the content and physical conditions of the interstellar medium (ISM). Absorption line spectroscopy can be used to study the ISM in our Galaxy, in nearby systems such as the Magellanic Clouds, and in the intergalactic medium out to the most distant QSOs. These studies provide an opportunity to compare elemental abundances and physical conditions in regions with differing chemical histories.

As part of a general program to investigate the interstellar medium of the Milky Way and nearby galaxies, we have used the *Far Ultraviolet Spectroscopic Explorer* (*FUSE*) satellite (Moos et al. 2000) to observe the star Sk -67 05 (HD 268605) in the Large Magellanic Cloud (LMC). The first observations of Galactic halo gas with IUE were along sightlines to stars in the LMC (Savage & de Boer 1979; 1981). In this Letter we discuss the first *FUSE* observations of an LMC star revealing O VI absorption in both the Milky Way and LMC. We also discuss the measurements of H₂, P II, Si II, Ar I, and Fe II absorption along this sightline.

2. OBSERVATIONS AND DATA PROCESSING

Sk -67 05 ($l = 278^\circ 89$, $b = -36^\circ 32$) is a B0 Ia star (Smith Neubig & Bruhweiler 1999) located near the western edge of the LMC. It lies in a diffuse H II region (Chu et al. 1994) with relatively low diffuse X-ray emission compared to regions closer to the center of the LMC (Snowden & Petre 1994). Ardeberg et al. (1972) give $B-V = -0.12$, and for $(B-V)_0 = -0.23$ (Binney & Merri-

field 1998), we find $E(B-V) = 0.11$. Using the Galactic gas-to-dust correlation (Dioplas & Savage 1994) we infer $N(\text{H I}) \sim 5.4 \times 10^{20} \text{ cm}^{-2}$ along this sightline.

This star was observed during the In-Orbit Checkout phase of the mission (Sahnow et al. 2000) at various times between 1999 August 20 and 1999 October 19. As these observations were part of tests designed primarily to align the four optical channels in the instrument, the star was stepped across the $30'' \times 30''$ aperture during the observations. However, the data were taken in time-tagged photon-address mode, so that corrections could be made for this image motion. The analysis here uses LiF1 (990 - 1080 Å) data only; the LiF2 channel has lower sensitivity and poorer flatfield characteristics, and during this period no flatfield corrections were available. The SiC (905 - 1100 Å) channels were generally not aligned. The instrument was still in its preflight focus configuration, and the spectral resolution was $\lambda/\Delta\lambda \lesssim 15,000$. The wavelength scale was established with a pre-flight dispersion solution. However, because of the stepping manner in which the data were obtained, additional zero point adjustments were required. Relative velocities are generally accurate to $\sim 10 \text{ km s}^{-1}$ over limited spectral ranges, and the absolute scale was set by comparison with IUE spectra. The data presented represent a total of approximately 33 ksec of on-target exposure time for the LiF1A and 35 ksec for the LiF1B spectral regions, approximately equally split between day and night. Additional details of the data processing for this data set can be found elsewhere (Massa et al. 2000).

This star exhibits variable stellar wind features. How-

¹Dept. of Physics & Astronomy, The Johns Hopkins University, Baltimore, MD 21218

²Dept. of Astronomy, University of Wisconsin, Madison, WI 53706

³Dept. of Astronomy & Astrophysics, University of Chicago, Chicago IL 60637

⁴Laboratory for Astronomy and Solar Physics, NASA/GSFC, Code 681, Greenbelt, MD 20771

⁵Institut d'Astrophysique de Paris, CNRS, 98 bis bld Arago, F-75014 Paris, France

⁶Center for Astrophysics and Space Astronomy, University of Colorado, CB 389, Boulder, CO 80309

ever, as shown in Figure 3 of Massa et al. (2000), the variability is minimal at the wavelengths of interest here, and does not affect our conclusions.

3. INTERSTELLAR ABSORPTION FEATURES

Figure 1 shows the composite spectrum from the LiF1 channel. Several metal lines that appear in the ISM of both the Milky Way and LMC are identified. Most other lines are due to H_2 absorption in the LMC. The strong emission line is terrestrial $Ly\beta$ $\lambda 1025.72$ airglow from the daytime exposures.

In this analysis we have used only the 1031.93 Å member of the O VI doublet since the 1037.62 Å line is blended with C II* 1037.02 Å and several H_2 lines. Figure 2 shows the *FUSE* O VI $\lambda 1031.93$ absorption line and a high-dispersion IUE spectrum of the C IV $\lambda 1550.77$. The H_2 (6-0) P(3) line originating in the LMC appears at +88 km s⁻¹, and must be modelled and removed to get an accurate estimate of the O VI column density.

We have analyzed the (2-0) to (9-0) H_2 Lyman bands, using the method described in Shull et al. (2000) to determine the equivalent widths, b -values, and column densities for the Milky Way and LMC components of H_2 . Since the typical spacing between the rotational-vibrational lines within each Lyman band is very close to the spacing between LMC and the Milky Way absorption, the measurement of the Milky Way H_2 depends on a careful decomposition of blended lines. Because of this difficulty, we used only the (4-0) and (2-0) Lyman bands to measure the $J = 0, 1$ levels from the Milky Way gas.

The results of the H_2 model, discussed below, give $\log N(H_2) = 15.28$ for the (6-0) P(3) in the LMC. This was convolved with the instrumental resolution of 25 km s⁻¹ and divided out of the original spectrum to remove the effects of the H_2 absorption. The resulting O VI profile is shown as a light line in Fig. 2.

To calculate the O VI absorption we have considered two possible continuum placements, designated “high” and “low,” which are displayed in Fig. 2 as long-dashed and dash-dotted lines, respectively. The arrow at +180 km s⁻¹ denotes the velocity we have adopted as separating the Milky Way and LMC components of O VI. Table 1 gives O VI equivalent widths derived using both continua.

Figure 3 shows the spectra of several important metal lines and a molecular hydrogen line along the sightline to Sk -67 05. For comparison, the IUE spectrum of Si II $\lambda 1808.01$ is shown. The individual absorption lines have separately been shifted in velocity to align the Milky Way components with the corresponding feature in the IUE spectrum. We established the velocity scale for the O VI region by shifting the Si II $\lambda 1020.70$ line to match the Si II $\lambda 1808.01$ IUE velocity scale, which sets the velocities of the nearby H_2 Lyman (7-0) P(2) $\lambda 1016.46$ and P(3) $\lambda 1019.50$ lines. The (6-0) P(3) $\lambda 1031.19$ and R(4) $\lambda 1032.35$ lines were then used to establish the O VI velocity, as shown in Fig. 2. The measured equivalent widths of several interstellar metal lines are also given in Table 1.

The adopted column densities for several ionic species, as well as several rotational states of H_2 along this sightline, are given in Table 2. These were calculated by fitting to a single-component Doppler-broadened curve of growth for Fe II and H_2 , and by using the apparent column density method (Savage & Sembach 1991) for the other species

listed. The two values given for the O VI column are based on the high and low continuum placements. We have added a systematic error of 0.04 dex in quadrature with the statistical error for O VI to account for errors in continuum placement and the velocity interval over which the apparent column density is integrated.

4. DISCUSSION

Since 114 eV are required to convert O⁺⁴ to O⁺⁵, O VI is almost never produced by photoionization from starlight. Thus, it is a sensitive tracer of hot ($\sim 300,000$ K) collisionally ionized gas in the interstellar medium. Adopting the high continuum placement shown in Fig. 2, which we believe is more appropriate, the O VI column density is $\log N(O VI) = 14.40 \pm 0.02$ and 13.89 ± 0.03 in the Milky Way and LMC, respectively. For the MW gas, $\log[N(O VI)\sin|b|] = 14.17$, which agrees well with the median value of 14.21 along 11 Galactic halo sightlines studied by Savage et al. (2000). Here $b = -36^\circ 32'$ is the galactic latitude.

Using $\log N(C IV) = 14.41$ in the Milky Way from Wakker et al. (1998) and assuming an error of 0.05 dex, we find $N(C IV)/N(O VI) = 1.00 \pm 0.16$. If the low continuum is adopted, this ratio is 1.23 ± 0.20 . Either value is greater than, but consistent with, the halo value $\langle N(C IV)/N(O VI) \rangle \sim 0.6$ determined from *FUSE* observations of four extragalactic sightlines (Savage et al. 2000), as well as $\langle N(C IV)/N(O VI) \rangle \sim 0.9$ from *Copernicus* and IUE observations of stars in the lower halo (Spitzer, 1996).

Note that the widths of O VI components in both the MW and LMC are much broader than the thermal line width, which is ≈ 30 km s⁻¹ (FWHM) for gas at 300,000 K. The substantial difference in the widths of the C IV and O VI lines may be due to the different scale heights in the Galactic halo of these ions (Savage et al. 2000).

Sk -67 05 was the only star for which Wakker et al. (1998) did not detect C IV in their study of the LMC halo. We recalculated their upper limit to $N(C IV)$ assuming the velocity range observed in the O VI gas (+180 to +322 km s⁻¹) and find $\log N(C IV) < 13.5$ (3σ). Adopting the high continuum case we find $N(C IV)/N(O VI) < 0.4$ (3σ) for the LMC material along the Sk -67 05 sightline.

The H_2 column density varies greatly between the LMC and Milky Way. For the LMC we find $\log N(H_2) = 19.50 \pm 0.08$, summed over the $J = 0$ to 5 states (Table 2), and a b -value of 5 ± 2 km s⁻¹. This column density is significantly higher than that measured along other LMC sightlines (de Boer et al. 1998; Shull et al. 2000). By comparison, *FUSE* observations of the metal deficient galaxy I Zw 18, have yielded only an upper limit, $\log N(H_2) \lesssim 15$ (Vidal-Madjar et al. 2000).

The distribution of H_2 rotational states in the LMC is best fitted by a two-component excitation temperature (Fig. 4) with $T_{01} = 59 \pm 5$ K for $J = 0, 1$ and $T_{ex} = 800 \pm 330$ K for $J = 3, 4, 5$. This is similar to the temperature distribution seen along the sightline to star LH10:3120 in the LMC using ORFEUS (de Boer et al. 1998). This indicates that the gas is not in thermal equilibrium, and the higher J states are fluorescently pumped by UV radiation. This excited gas may therefore exist in the outer, optically thin regions of the cloud. In the interior regions the molecular fraction may increase due

to self-shielding, which is expected when $E(B-V) \gtrsim 0.1$ (Savage et al. 1977). The $J = 2$ point falls almost exactly on the extension of the T_{01} line, suggesting that the density of this gas is rather high.

For the Milky Way gas we find an H_2 column density of $\log N(H_2) = 14.95 \pm 0.08$, summed over the $J = 0$ to 3 states (Table 2), and a rotational temperature of $T_{01} = 99^{+30}_{-20}$ K (Fig. 4). This temperature is similar to other values measured with *FUSE* (Shull et al. 2000) and to *Copernicus* measurements of Galactic stars (Savage et al. 1977). There is an indication of a two-component temperature distribution for the Milky Way gas as well. However, because of the relatively small number of measurable lines and severe blending, we are unable to accurately determine an excitation temperature for the higher- J MW material.

Absorption from both Milky Way and LMC material is clearly seen in all of the low ions present in the LiF1 data (e.g., Figs. 1 and 3). Blending of atomic, ionic, and H_2 absorption along this sightline limits the number of species for which we can derive accurate equivalent widths and column densities. The depleted species Fe II has several well-observed transitions in our dataset (Table 1). We have constructed a single-component Doppler-broadened curve of growth for the Fe II lines observed in both the Milky Way and the LMC. The best fit yields $\log N(\text{Fe II}) = 14.8 \pm 0.1$ and 14.8 ± 0.1 with $b = 14.2 \pm 0.5$ and $12.1^{+2.1}_{-1.6}$ km s $^{-1}$ for the Milky Way and LMC, respectively. Due to potential uncertainties in some of the f -values we have adopted a conservative error of 0.1 dex in these column densities. Our data permit good measurements of the non-depleted species P II $\lambda 1152.82$, and we derive lower limits to the Milky Way and LMC column densities (Table 2) using the apparent column density method of Savage & Sembach (1991). If the b -values for P II are similar to those derived for Fe II, the data suggest only very moderate saturation corrections of $\lesssim 0.1$ dex.

For the sightline through the halo of the Milky Way, we derive a gas-phase abundance $[\text{Fe}/\text{P}] \equiv \log N(\text{Fe II}) - \log N(\text{P II}) - \log(\text{Fe}/\text{P})_{\odot} \sim -0.6$, assuming a solar system ratio of $\log(\text{Fe}/\text{P})_{\odot} = +1.92$ (Anders & Grevesse 1989). For the LMC gas along this direction we find $[\text{Fe}/\text{P}] \sim -0.7$. This suggests significant incorporation of iron into dust grains in both galaxies. Differences in the

relative abundance of singly- and doubly-ionized iron and phosphorous could affect this measurement (Sembach et al. 2000), but the magnitude of this effect is likely to be much too small to account for the gas-phase deficiency of iron along this sightline. The derived values of $[\text{Fe}/\text{P}]$ are similar to the values of $[\text{Fe}/\text{Zn}] = -1.06$ and -0.91 for the Milky Way halo and LMC absorption towards SN 1987A (Welty et al. 1999). Future *FUSE* observations of a large number of LMC sightlines will allow us to study the distribution of gas-phase abundances and infer the composition of interstellar dust in this environment.

5. SUMMARY

We have reported equivalent widths and column densities of O VI, H_2 , P II, Si II, Ar I, and Fe II along the line of sight to Sk -67 05 in the LMC using *FUSE* data. The principal results of this study are:

1. In the halo of the Milky Way toward the LMC $N(\text{C IV})/N(\text{O VI}) = 1.00 \pm 0.16$, a value somewhat greater than but consistent with other *FUSE* observations through the halo (Savage et al. 2000). In the LMC, where only an upper limit on $N(\text{C IV})$ is available, we find $N(\text{C IV})/N(\text{O VI}) < 0.4$ (3σ). This is consistent with the lower ratio seen in the disk of the Milky Way compared to the halo (Savage et al. 2000; Spitzer 1996).
2. The LMC is rich in H_2 along this sightline, $\log N(H_2) = 19.50 \pm 0.08$. A two-component temperature fit gives $T_{01} = 59 \pm 5$ K for and $T_{ex} = 800 \pm 330$ K.
3. The gas-phase abundances of $[\text{Fe}/\text{P}] \sim -0.6$ and ~ -0.7 in the Milky Way and LMC suggests significant depletion in both locations relative to solar abundances.

We thank D. Massa for providing the software to co-add the spectra used in this analysis. This work is based on data obtained for the Guaranteed Time Team by the NASA-CNES-CSA *FUSE* mission operated by the Johns Hopkins University. Financial support to U. S. participants has been provided by NASA contract NAS5-32985

REFERENCES

- Anders, E. & Grevesse, N. 1989, *Geochim. Cosmochim. Acta*, 53, 197
 Binney, J. & Merrifield, M. 1998, *Galactic Astronomy*, Princeton University Press.
 de Boer, K. S., Richter, P., Bomans, D. J., Heithausen, A., & Koorneef, J. 1998, *A&A*, 338, L5
 Chu, Y.-H., Wakker, B., Mac Low, M.M., Garcia-Segura, G. 1994, *AJ*, 108, 1696
 Diplas, A. & Savage, B. D. 1994, *ApJ*, 427, 274.
 Massa, D. et al. 2000, *ApJ*, this issue
 Moos, H. W. et al. 2000, *ApJ*, this issue
 Sahnou, D. J. et al. 2000, *ApJ*, this issue
 Savage, B. D., Bohlin, R. C., Drake, J. F., & Budich, W. 1977, *ApJ*, 216, 291
 Savage, B. D. & de Boer, K. S. 1979, *ApJ*, 230, L77
 Savage, B. D. & de Boer, K. S. 1981, *ApJ*, 243, 460
 Savage, B. D. & Sembach, K. R. 1991, *ApJ*, 379, 245
 Savage, B. D. et al. 2000, *ApJ*, this issue
 Sembach, K. R., Howk, J. C., Ryans, R. S., & Keenan, F. P. 2000, *ApJ*, 528, 310
 Shull, J. M. et al. 2000, *ApJ*, this issue
 Smith Neubig, M. M., & Bruhweiler, F. C. 1999, *AJ*, 117, 2856
 Snowden, S. L., & Petre, R. 1994, *ApJ*, 436, 123
 Spitzer, L. 1996, *ApJ*, 458, L29
 Vidal-Madjar, A. et al. 2000, *ApJ*, this issue
 Wakker, B. P., Howk, J. C., Chu, Y.-H., Bomans, D., & Points, S. D. 1998, *ApJ*, 499, L87
 Welty, D. E., Frisch, P. C., Sonneborn, G., & York, D. G. 1999, *ApJ*, 512, 636

TABLE 1
IONIC EQUIVALENT WIDTHS

Ion	λ	$\log \lambda f$	W_λ [mÅ] ^a	
			MW	LMC
O VI	1031.926	2.14	249 ± 10^b	87 ± 5^b
	1031.926	2.14	213 ± 8^c	...
Si II	1020.699	1.46	99 ± 3	143.0 ± 2.4
P II	1152.818	2.43	74.3 ± 2.1	78.6 ± 1.7
Ar I	1048.220	2.41	127.0 ± 2.2	105.2 ± 2.4
Fe II	1055.262	0.81	...	31.0 ± 1.9
Fe II	1112.048	0.84^d	...	34.5 ± 1.9
Fe II	1121.975	1.35^d	85.4 ± 1.9	81 ± 3
Fe II	1125.448	1.24	77.8 ± 2.3	66.7 ± 2.3
Fe II	1127.098	0.48^d	16.2 ± 1.9	11.2 ± 1.1
Fe II	1133.665	0.74	38 ± 5	...
Fe II	1142.366	0.63	16 ± 3	...
Fe II	1144.938	2.10	173 ± 4	...

^aMeasured equivalent widths and 1σ uncertainties (in mÅ) for the Milky Way (MW) and LMC components towards Sk-67 05.

^bDerived using the “high” continuum (see text).

^cDerived using the “low” continuum (see text). Probable contamination from H₂ (6 – 0) P(3) 1031.19 Å line removed.

^dOscillator strength taken from the preliminary results of Howk et al. (2000, in preparation).

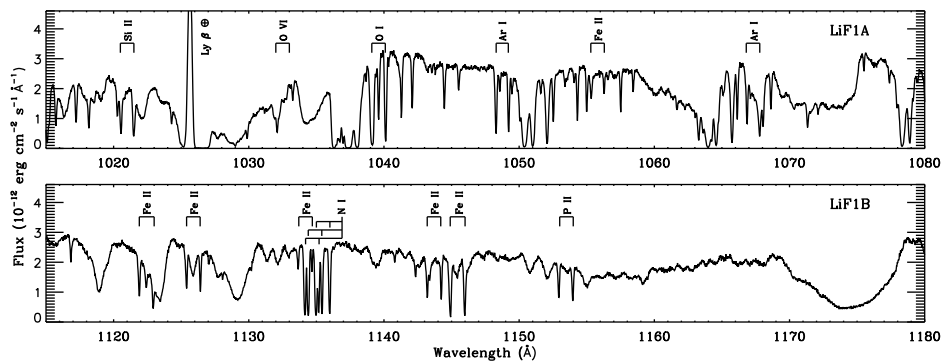


FIG. 1.— The composite LiF1A and LiF1B spectra of Sk -67 05. Several important metal lines having components in both the Milky Way and LMC are marked. Most of the other absorption lines are due to molecular hydrogen in the LMC. The strong emission line at 1025.72 Å is due to terrestrial Ly β airglow. The fully sampled data has been smoothed by four pixels in these plots. This smoothing does not affect the observed linewidths because the data are oversampled.

TABLE 2
ADOPTED COLUMN DENSITIES

Species	$\log N$ [cm ⁻²] ^a		Method ^b
	MW	LMC	
O VI	14.40 ± 0.02^c	13.89 ± 0.03^c	1
O VI	14.32 ± 0.02^d	...	1
P II	$\gtrsim 13.5$	$\gtrsim 13.6$	1
Si II	$\gtrsim 13.9$	$\gtrsim 14.5$	1
Ar I	$\gtrsim 14.0$	$\gtrsim 13.8$	1
Fe II	14.8 ± 0.1	14.8 ± 0.1	2
H ₂ ($J = 0$)	14.26 ± 0.09	19.34 ± 0.10	2
H ₂ ($J = 1$)	14.46 ± 0.08	18.99 ± 0.10	2
H ₂ ($J = 2$)	$14.41^{+0.15}_{-0.21}$	$16.28^{+0.30}_{-0.50}$	2
H ₂ ($J = 3$)	$14.23^{+0.13}_{-0.19}$	$15.28^{+0.30}_{-0.50}$	2
H ₂ ($J = 4$)	...	14.46 ± 0.06	2
H ₂ ($J = 5$)	...	$14.62^{+0.18}_{-0.30}$	2

^aLogarithm of the adopted column densities for the Milky Way (MW) and LMC components towards Sk-67 05 (in units of ions cm⁻²).

^bMethod used for deriving column densities: (1) Apparent column density method; (2) Curve of growth fitting method.

^cColumn density using “high” continuum (see text).

^dColumn density using “low” continuum (see text).

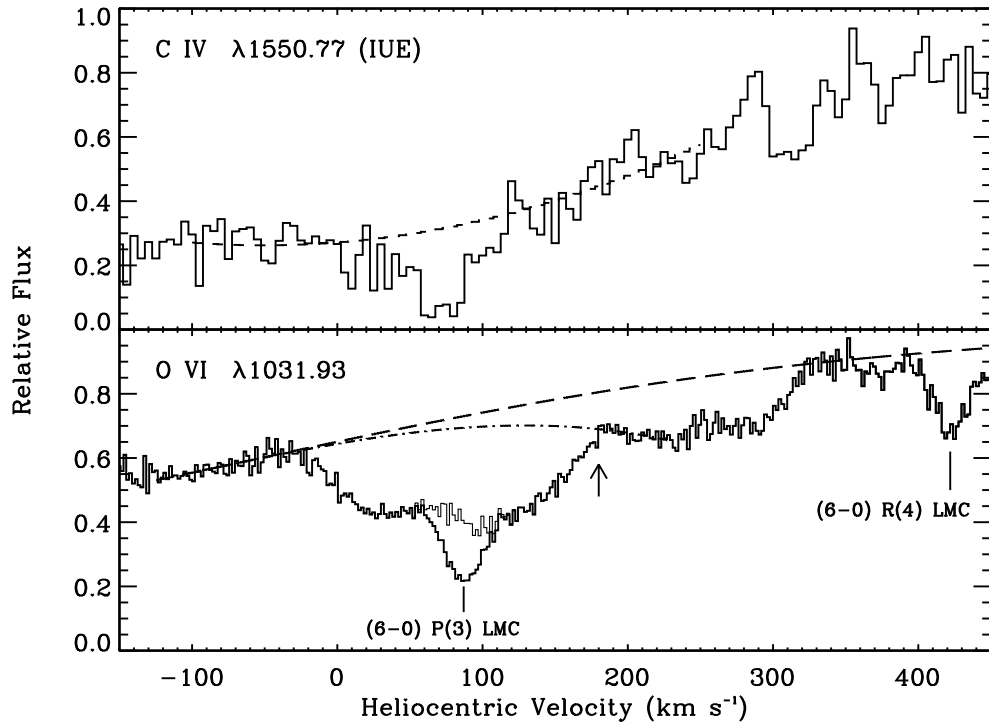


FIG. 2.— The O VI 1031.93 Å line profile from *FUSE* and the C IV 1550.77 Å line profile from IUE. The velocity scale has been adjusted as described in the text. Both “high” (long-dashed line) and “low” (dashed-dotted line) continuum placements have been considered in the O VI analysis. The arrow denotes the adopted division between the Milky Way gas at velocities $< 180 \text{ km s}^{-1}$ and the LMC gas at velocities $> 180 \text{ km s}^{-1}$. The H₂ (6 – 0) P(3) line, arising in the LMC, falls directly in the Milky Way O VI absorption line. The model fit has been divided out to remove the effects of the H₂ absorption, and the resulting O VI profile is shown as a light line.

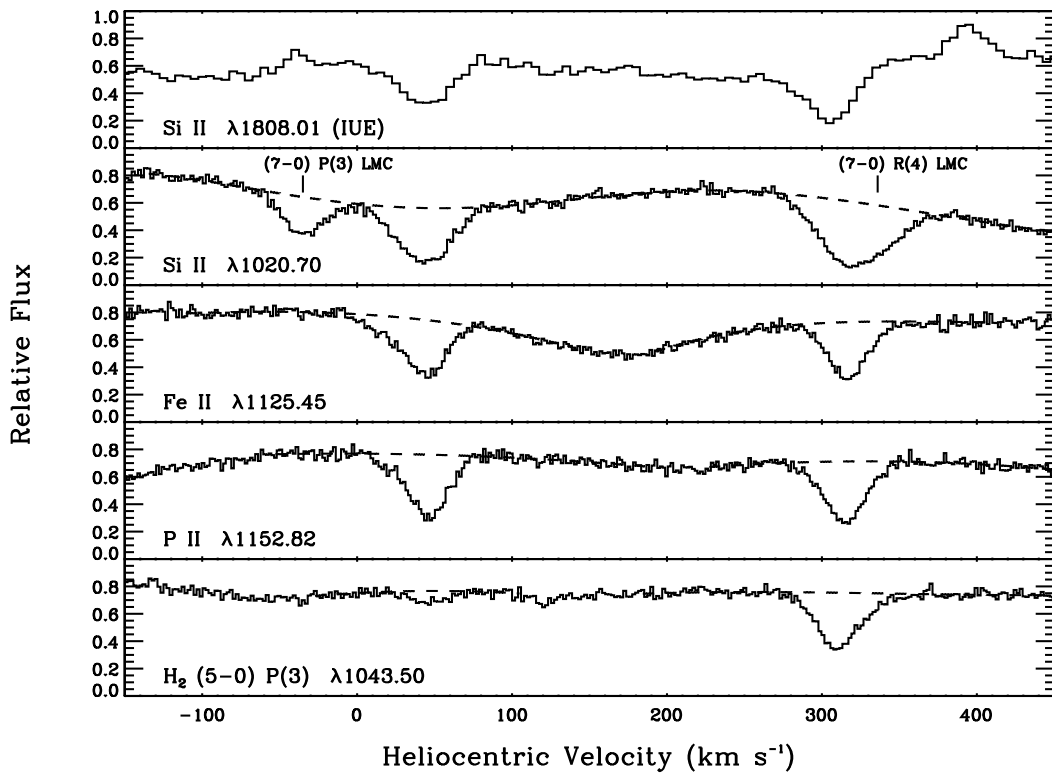


FIG. 3.— Selected absorption lines of low ions in the *FUSE* bandpass, together with the Si II 1808.01 Å line from IUE observations. Dashed lines show the adopted continuum levels. The equivalent widths of the MW and LMC components are given in Table 1. The velocity scales of the *FUSE* lines have been adjusted to make the Milky Way component velocities match that of the Si II IUE line. The LMC component of Si II $\lambda 1020.70$ is broadened due to a blend with the indicated H_2 line.

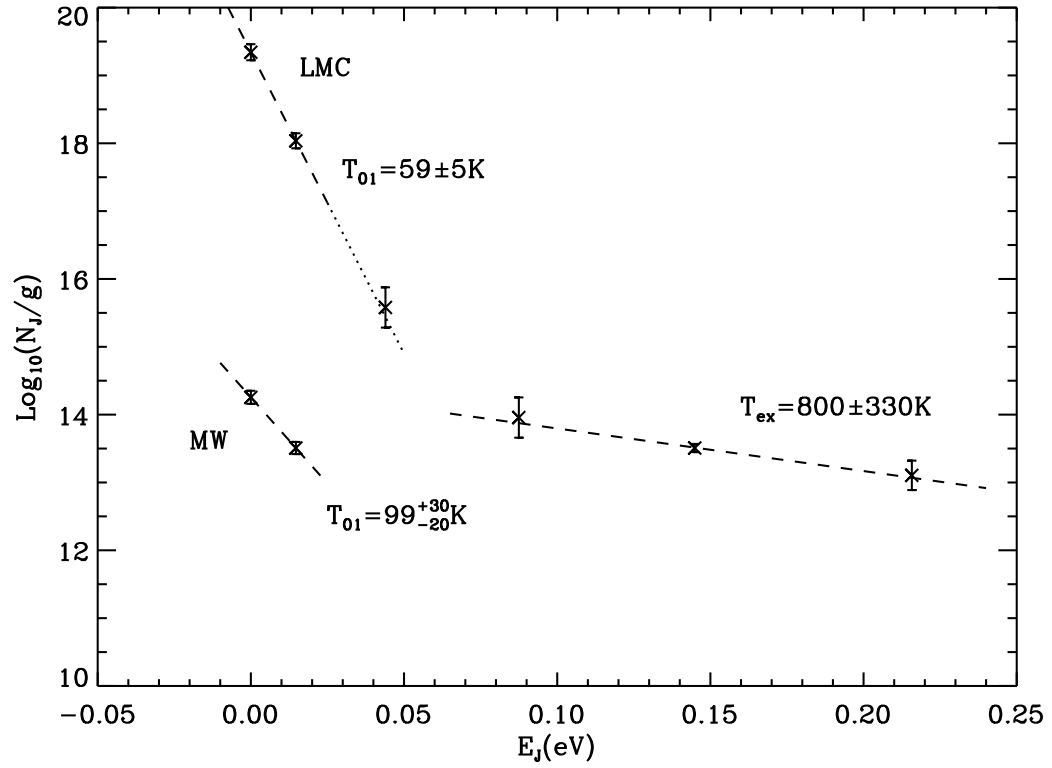


FIG. 4.— Column densities for the $J=0-5$ levels of H_2 in the LMC and Milky Way. For the LMC a two-component fit is possible, with the excitation temperatures indicated. For the much weaker Milky Way lines, reliable column densities could only be determined for the $J=0$ and 1 levels. Note that the dotted line extension of the LMC T_{01} line intersects the $J=2$ point, indicating that the density of this gas is rather high. The LMC H_2 column densities shown here are significantly higher than those reported along other LMC sightlines (de Boer et al. 1998; Shull et al. 2000).